



Development and Validation of a Novel Mitochondrion and Ferroptosis-Related Long Non-Coding RNA Prognostic Signature in Hepatocellular Carcinoma

Wuzheng Xia^{1,2†}, Cong Zeng^{1,3†}, Zehao Zheng^{2,4†}, Chunwang Huang^{5*}, Yu Zhou^{6*} and Lan Bai^{1*}

OPEN ACCESS

Edited by:

Hai-Feng Zhang,
Sun Yat-sen Memorial Hospital, China

Reviewed by:

Li Tengcheng,
Third Affiliated Hospital of Sun Yat-sen
University, China
Le Wang,
Third Affiliated Hospital of Guangzhou
Medical College, China

*Correspondence:

Lan Bai
bailan_99@yeah.net
Yu Zhou
zhouyu@gdph.org.cn
Chunwang Huang
huangchunwang@126.com

[†]These authors have contributed
equally to this work

Specialty section:

This article was submitted to
Cell Death and Survival,
a section of the journal
Frontiers in Cell and Developmental
Biology

Received: 28 December 2021

Accepted: 20 June 2022

Published: 12 August 2022

Citation:

Xia W, Zeng C, Zheng Z, Huang C,
Zhou Y and Bai L (2022) Development
and Validation of a Novel
Mitochondrion and Ferroptosis-
Related Long Non-Coding RNA
Prognostic Signature in
Hepatocellular Carcinoma.
Front. Cell Dev. Biol. 10:844759.
doi: 10.3389/fcell.2022.844759

¹Guangdong Provincial Key Laboratory of Gastroenterology, Department of Gastroenterology, Nanfang Hospital/The First School of Clinical Medicine, Southern Medical University, Guangzhou, China, ²Department of Organ Transplant, Guangdong Provincial People's Hospital, Guangdong Academy of Medical Sciences, Guangzhou, China, ³Department of General Practice, Hospital of South China Normal University, Guangzhou, China, ⁴Department of General Surgery, Shantou University of Medical College, Shantou, China, ⁵Department of Ultrasound, Guangdong Provincial People's Hospital, Guangdong Academy of Medical Sciences, Guangzhou, China, ⁶Department of Pancreatic Surgery, Department of General Surgery, Guangdong Provincial People's Hospital, Guangdong Academy of Medical Sciences, Guangzhou, China

Mitochondrion and ferroptosis are related to tumorigenesis and tumor progression of hepatocellular carcinoma (HCC). Therefore, this study focused on exploring the participation of lncRNAs in mitochondrial dysfunction and ferroptosis using public datasets from The Cancer Genome Atlas (TCGA) database. We identified the mitochondrion- and ferroptosis-related lncRNAs by Pearson's analysis and lasso-Cox regression. Moreover, real-time quantitative reverse transcription PCR (RT-qPCR) was utilized to further confirm the abnormal expression of these lncRNAs. Based on eight lncRNAs, the MF-related lncRNA prognostic signature (LPS) with outstanding stratification ability and prognostic prediction capability was constructed. In addition, functional enrichment analysis and immune cell infiltration analysis were performed to explore the possible functions of lncRNAs and their impact on the tumor microenvironment. The pathways related to G2M checkpoint and MYC were activated, and the infiltration ratio of regulatory T cells and M0 and M2 macrophages was higher in the high-risk group. In conclusion, these lncRNAs may affect mitochondria functions, ferroptosis, and immune cell infiltration in HCC through specific pathways, which may provide valuable insight into the progression and therapies of HCC.

Keywords: lncRNAs, mitochondrion, ferroptosis, signature, hepatocellular carcinoma

INTRODUCTION

Hepatocellular carcinoma (HCC) accounts for 80% of the primary liver tumors and is one of the most common malignant cancers in the world (Petrick et al., 2016). From 1990 to 2017, the mortality of HCC in China increased by 50% (from 20 to 30 death per 100,000) (Zhou et al., 2019). Surgical therapies (included surgical resection and liver transplantation) and tumor ablation are recommended as potential curative methods by several guidelines (Heimbach et al., 2018; Zhou

et al., 2019; Benson, 2021). Most of the treatments can achieve excellent long-term survival but still remained unsatisfactory (Ishizawa et al., 2008; Bruix et al., 2016; Lencioni et al., 2016). Therefore, it is urgent to figure out the new therapeutic targets for hepatocellular carcinoma.

As a vital cellular organelle, the mitochondrion plays an important role in several crucial cellular activities, such as biosynthesis, signaling, and apoptosis (Zong et al., 2016; Yuan et al., 2020). Studies have shown that the mitochondrion can also have pivotal influence in cell fate decision (Shyh-Chang et al., 2013; Bahat and Gross, 2019). Moreover, current evidences indicate that mitochondrial defects are related to tumor growth and cell proliferation (Zheng et al., 2013; Zong et al., 2016; Li et al., 2020). Thus, mitochondrion and mitochondrial functions are regarded as potential therapeutic targets for several malignancies.

Dysfunction of iron metabolism is associated with tumorigenesis and tumor cell proliferation (Manz et al., 2016). Moreover, excessive intracellular iron accumulation and massive lipid peroxidation can impact the fate of the cell and lead to ferroptosis (Gao et al., 2019; Li et al., 2021). Ferroptosis is an iron-dependent and non-apoptotic-regulated cell death (Stockwell et al., 2017; Tang et al., 2021). At present, inducing ferroptosis of tumor cells is considered to be one of the promising directions for the treatment for several tumors (Hassannia et al., 2019).

Long noncoding RNAs (lncRNAs) are a heterogeneous group of non-protein-coding transcripts with lengths of greater than 200 nucleotides (Prensner and Chinnaiyan, 2011; Dhanoa et al., 2018). lncRNAs are broadly classified into sense intronic RNA, antisense RNAs, long intergenic RNAs (lincRNAs), and bidirectional RNAs (Ahadi, 2021). lncRNAs can promote tumorigenesis, cell proliferation, migration, metastasis, and other important biological processes by regulating gene expression on epigenetic modification (Nandwani et al., 2021). A recent study has found that lncRNA MT1DP elevates ferroptosis *via* downregulating NRF2 in NSCLC cells (Gai et al., 2020). Another study shows that lncRNA MALAT1 regulates metabolic reprogramming through mitochondrial metabolism (Zhao et al., 2021). These research studies indicate that lncRNAs may have diagnostic and prognostic potentials for HCC patients (Lanzafame et al., 2018; Zhang et al., 2020). However, it remains unclear about how the lncRNAs affect the HCC cell fate by regulating the mitochondrial defects and ferroptosis.

In this study, we focused on exploring the participation of lncRNAs in mitochondrial dysfunction and ferroptosis. We identified eight mitochondrion and ferroptosis-related lncRNAs by Pearson's analysis, Lasso-Cox regression, and RT-qPCR. Based on these lncRNAs, the MF-related lncRNA prognostic signature (LPS) was constructed. This LPS had very outstanding stratification ability and prognostic prediction capability. In addition, function enrichment analysis and immune cell infiltration analysis were performed to explore the possible functions of lncRNAs and their impact on the tumor microenvironment.

TABLE 1 | Clinical characteristics of HCC patients in the training cohort and validation cohort.

Variables	No. of patients	
	Training	Validation
Gender		
Male	158	78
Female	72	40
Age		
≥60	128	59
<60	102	59
Tumor stage		
Stage I	103	59
Stage II	49	29
Stage III	58	24
Stage IV	3	1
unknown	17	5
T stage		
T1	107	63
T2	56	30
T3	55	22
T4	10	3
N stage		1
0	158	85
1	1	2
unknown	71	31
M stage		
M0	162	86
M1	3	1
unknown	65	31

MATERIALS AND METHODS

Datasets and Patients

The hepatocellular carcinoma RNA transcriptome raw count data (LIHC) and their clinicopathological characteristic information were downloaded from The Cancer Genome Atlas database (TCGA, <https://portal.gdc.cancer.gov/>). Those patients were included who (1) only underwent surgical resection; (2) pathologically diagnosed HCC; (3) survival longer than 30 days were included in this study. The patients from TCGA were randomly divided at a ratio of 2:1 into the training set ($n = 230$) and validation set ($n = 118$). The clinicopathological characteristic information for the TCGA LIHC including in this study is listed in **Table 1**.

Mitochondrion and Ferroptosis-Related Long Non-Coding RNA

The GENCODE website is an online database that integrates human and mouse gene annotations, including protein-coding RNAs, non-coding RNAs, and pseudogenes (Uszczynska-Ratajczak et al., 2018; Frankish et al., 2019). After downloading the lncRNA annotation file from the GENCODE website and recognizing the Ensemble ID of the gene in the TCGA LIHC dataset, all the lncRNAs were extracted. Differentially expressed lncRNAs were identified with the help of R packages *Deseq2* (Love et al., 2014). Cox proportional hazards regression was used to evaluate the prognostic value of these differentially expressed lncRNAs. According to previous

articles, 1136 mitochondrial genes and 116 ferroptosis genes were selected (**Supplementary Table S1**), and their expression values were extracted from the TCGA LIHC dataset (Du and Zhang, 2020; Chen et al., 2021a; Rath et al., 2021; Zhou et al., 2021, 2021). The R package *corrplot* was used to evaluate the correlations between genes and lncRNAs and calculated the correlation coefficient and *p* value. In this study, MF-related lncRNAs were defined as absolute correlation coefficient >0.5 and *p* value < 0.05.

Constructing and Validating the Mitochondrion and Ferroptosis-Related Long Non-Coding RNAs Prognostic Signature

With the help of *Glmnet* and *survival* R packages (Engelbrechtsen and Bohlin, 2019), eight MF-related prognostic lncRNAs were identified by least absolute shrinkage and selection operator (LASSO)-Cox regression analysis and RT-qPCR from 48 MF-related lncRNA and a MF-related lncRNA prognostic signature (LPS) was constructed (Tibshirani, 1997). The MF-related LPS risk score calculation formula was listed as follows:

$$Riskscore = \sum_{i=0}^n \beta_i * x_i$$

β_i was the coefficient and the x_i was the expression of lncRNA_{*i*}. Based on this formula, the risk score was calculated for each HCC patient.

Multiple Cox regression was utilized to identify the independent risk factors. The discrimination performance of the MF-related LPS was assessed by the area under the receiver operating characteristic (ROC) curve (AUC). Log-rank tests and Kaplan–Meier analyses were performed to assess the predictive ability and stratification ability of MF-related LPS and the independent risk factors. Overfit bias was decreased by bootstrap validation including 1000 resamples.

Function Enrichment Analysis for the DEG Between the High-Risk and Low-Risk Group

To explore the mechanisms of different prognosis between low-risk and high-risk groups, differential analysis was performed based on the “Deseq2” package and only when the adjusted *p*-value <0.05 and |logarithmic fold-change (logFC)| >1.5 were statistically significant (Yang et al., 2019). Gene Ontology (GO), Kyoto Encyclopedia Genes and Genomes (KEGG), and gene set enrichment analysis of the DEGs were performed by R package cluster Profiler (Yu et al., 2012). We investigated the biological meaning of the common DEGs thorough GO analyses. It focused on the biological process and cellular components (CC). Kyoto Encyclopedia Genes and Genomes (KEGG) and gene set enrichment analysis (GSEA) helped us identify and evaluate the potential mechanisms and pathways.

Correlation Analysis of the Mitochondrion and Ferroptosis-Related Prognostic Long Non-Coding RNA Signature and Immune Cell Infiltration

To assess the relationship between immune cell infiltration and our MF-related LPS, we performed the ESTIMATE analysis, EPIC analysis, and CIBERSORT algorithm (Chen et al., 2018; Racle and Gfeller, 2020). In addition, the Wilcoxon signed rank test was used to evaluate the proportion of immune cells between the high- and low-risk groups.

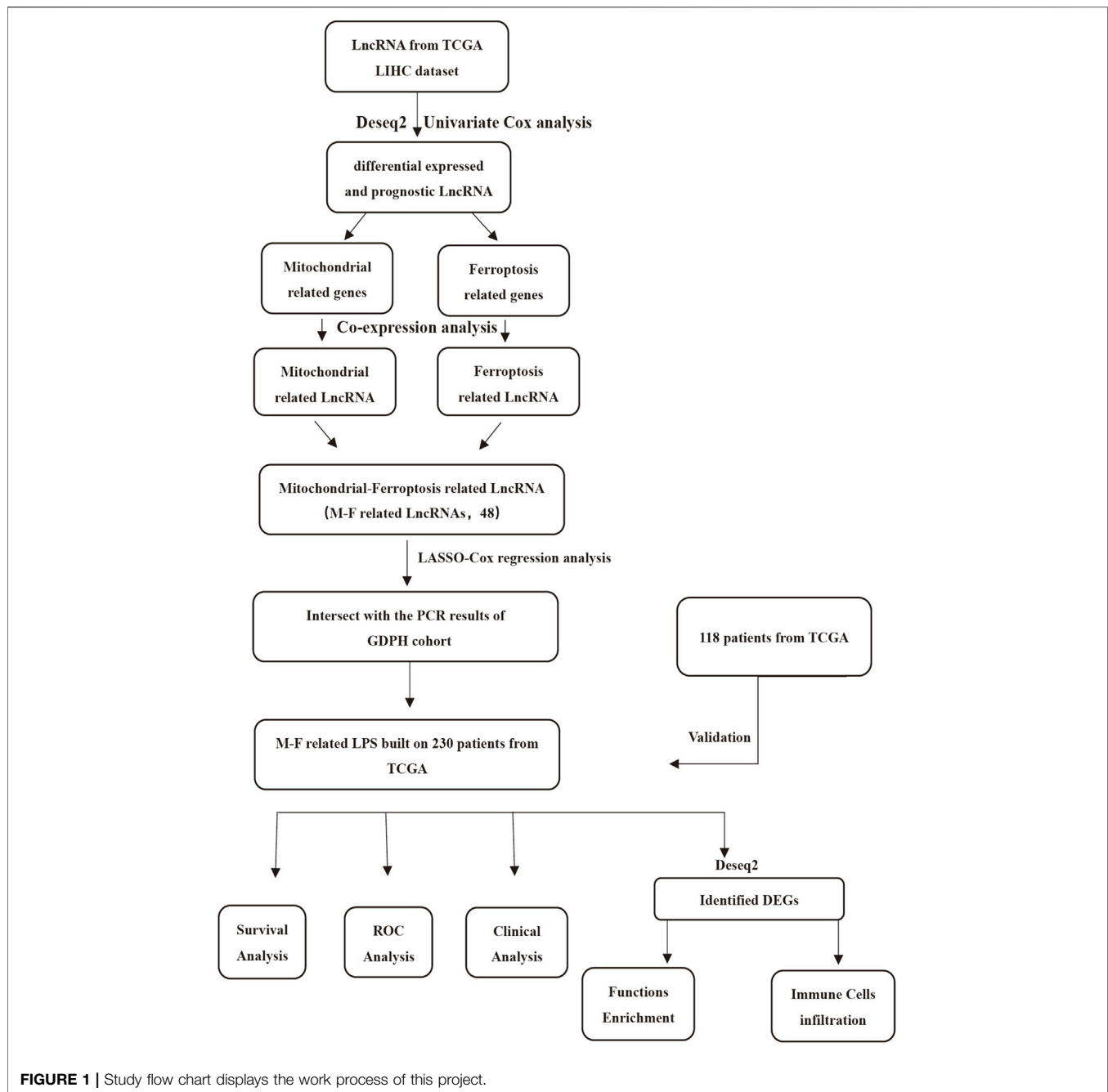
Tissue Specimen and Real-Time Quantitative Polymerase Chain Reaction

Thirty pair samples of hepatocellular carcinoma and adjacent normal tissues were collected from Guangdong Provincial People’s Hospital (GDPH). The samples were immediately frozen after surgical resection and preserved in liquid nitrogen at –80°C. This study is approved by the Research Ethics Committee of Guangdong Provincial People’s Hospital.

Real-time quantitative polymerase chain reaction (RT-qPCR) was utilized to evaluate the lncRNA expression. All the samples were extracted using TRIzol reagent RNA TRIpure reagent (Aidlab Biotechnologies, RN01). cDNA was prepared using RevertAid Reverse Transcriptase (Thermos Fisher, United States). Real-time quantitative PCR was performed by the AceQ Universal SYBR qPCR Master Mix Kit. GAPDH was used for internal control. Each sample was tested in triplicate at least three times. All fold-changes were calculated through relative quantification $2^{-(\Delta\Delta Ct)}$ [(GAPDH_{Cq}) – (lncRNA_{Cq})]. The detailed primers sequences are provided in **Supplementary Table S2**.

Statistical Analyses

Most statistical analyses were performed by R version 4.0.0 software (<http://www.r-project.org/>). The Deseq2 package was used to identify the differentially expressed lncRNA in the TCGA LIHC dataset. Cutoff values for the MF-related prognostic lncRNA and the nomogram were all defined by the receiver operating characteristic curve (ROC) analyses. Sangerbox, a useful and free online data analysis platform (<http://www.sangerbox.com/tool>), was used to analyze the correlation between the expression of 8 MF-related lncRNAs and clinicopathological factors. Kaplan–Meier analysis was used to compare the overall survival between the high-risk group and low-risk group. Univariate and multivariate Cox proportional hazards models were used to determine significant prognostic factors. The ROC curve was used to evaluate the predictive efficiency of the 8 MF-lncRNA. The figures of Kaplan–Meier analysis and ROC curves were drawn by Sangerbox platform. A *p* < 0.05 was considered statistically different.



RESULTS

Patient Clinicopathologic Characteristics

The flow chart (Figure 1) displays the work process of this project. Based on the criteria, 348 patients from the TCGA LIHC dataset were included in our study. The clinical data showed that the training set included 158 males and 72 females, while the validation set included 78 males and 40 females. The patients' age of the training set and validation set ranged from 16 to 90. The overall survival of all the patients was longer than 30 days. Approximately, 66.1% patients in

training cohorts and 74.6% patients in validation cohorts were at tumor stage I–II. Patient clinicopathologic characteristics are listed in Table 1.

Identification of the Mitochondrion and Ferroptosis-Related in LIHC Patients

The expression value of 12,079 lncRNAs was extracted from the TCGA LIHC dataset. We identified 2248 lncRNAs (1829 upregulated and 419 downregulated) that were differentially expressed in the TCGA-LIHC dataset

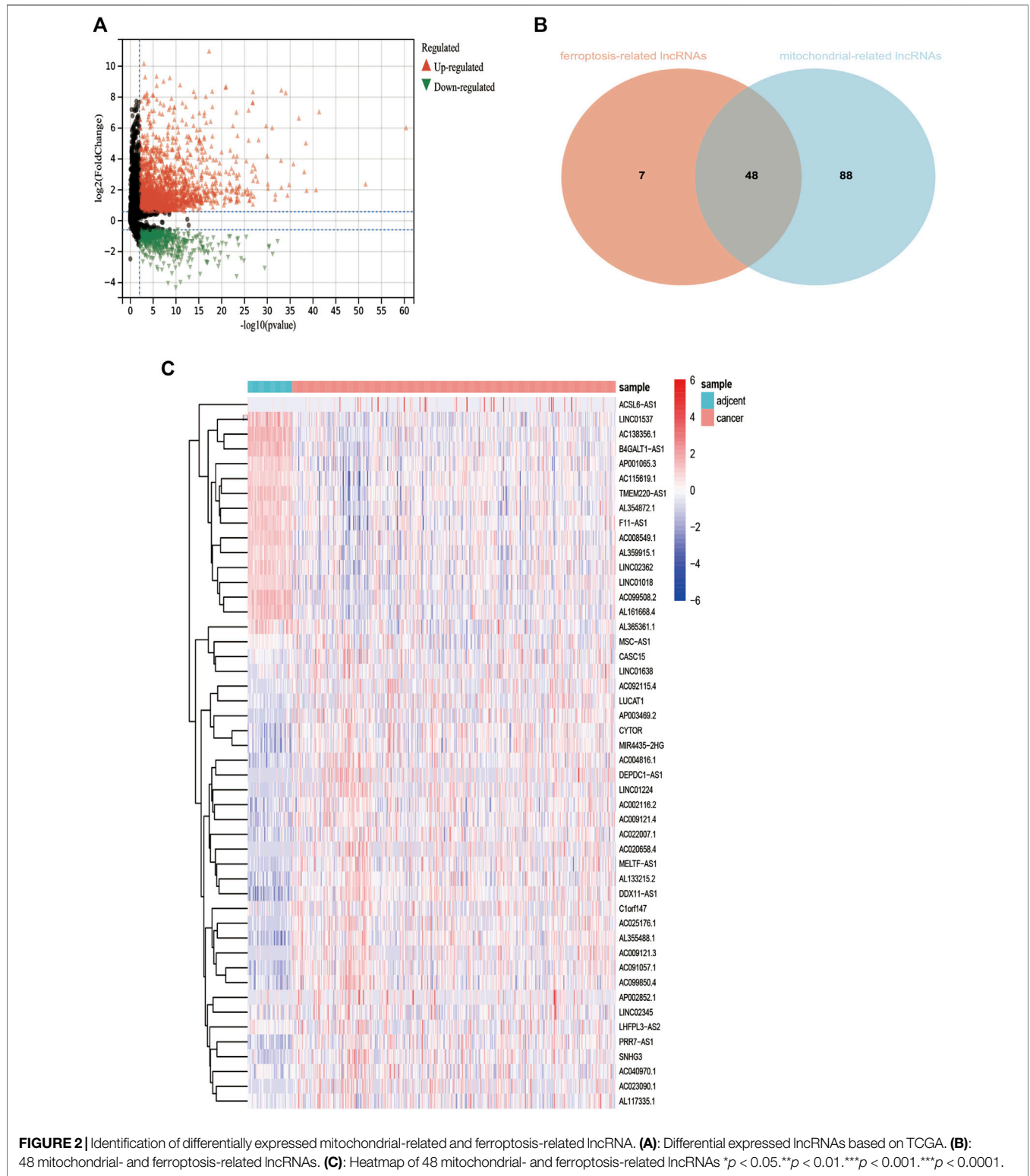
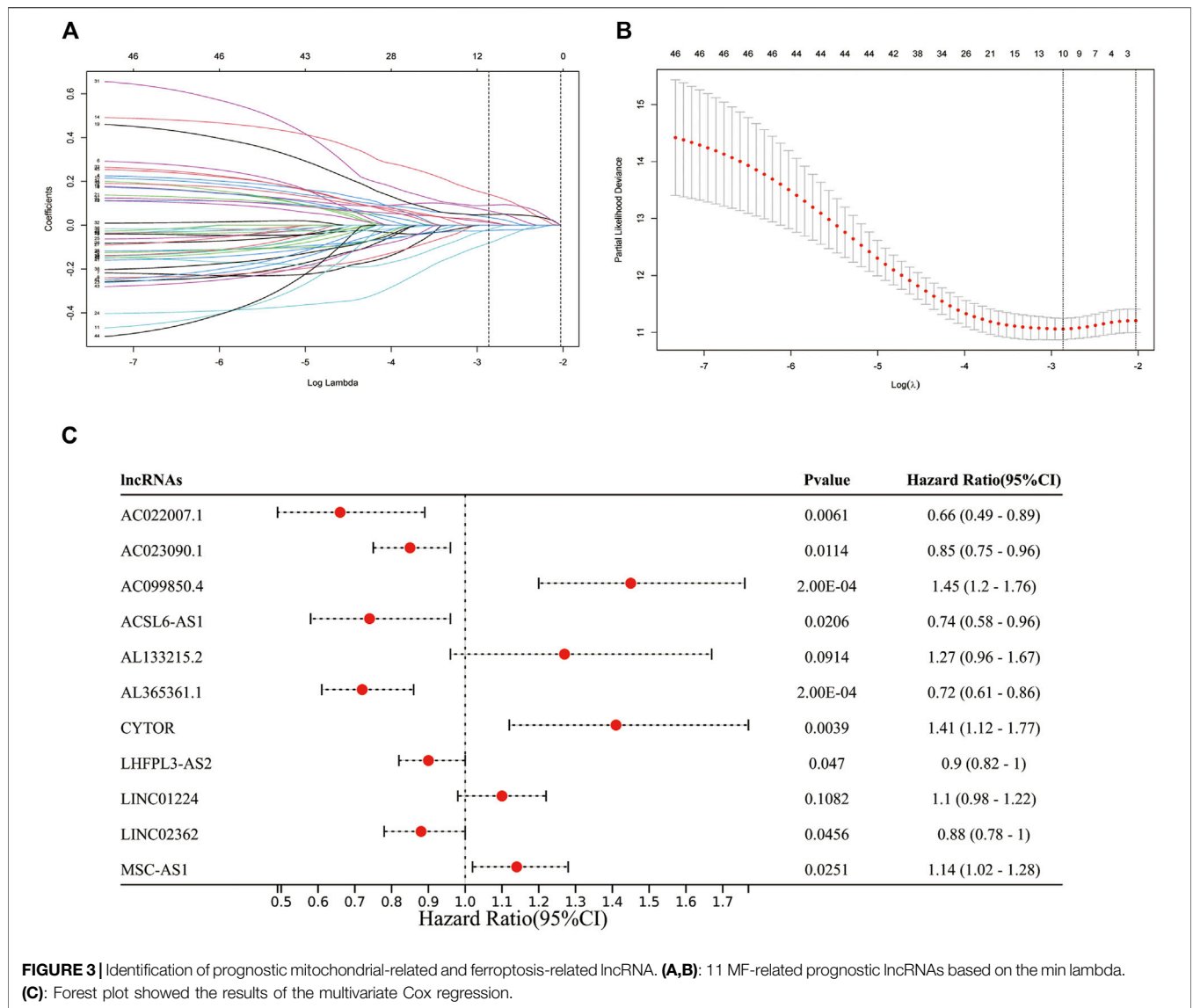


(Figure 2A). Univariate Cox regression analysis was performed to further estimate the impact of all the lncRNAs on the overall survival of LIHC patients in TCGA. Approximately, 404 differentially expressed and potential prognostic lncRNAs

were screened out. By using R package corrplot, Pearson’s correlation analysis was performed to calculate the correlations between the expression of mitochondrial genes or ferroptosis genes and differentially expressed and prognostic lncRNA in the



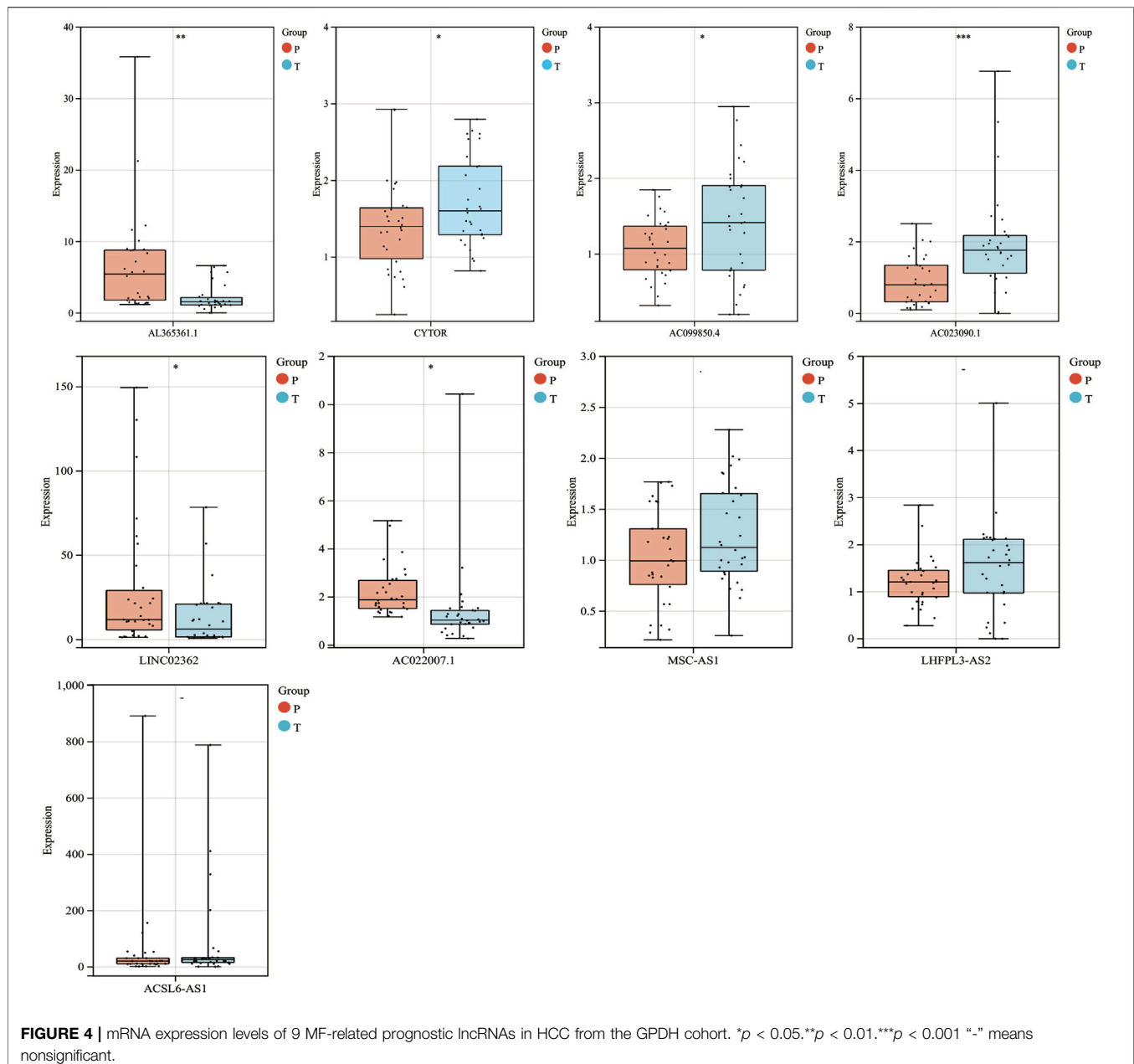
TCGA dataset. The lncRNA whose | Pearson R| > 0.5 and p < 0.05 was regarded as a mitochondrial-related or ferroptosis-related lncRNA. Subsequently, Venn analysis between the differential and prognostic mitochondrial-related lncRNAs and differential and prognostic ferroptosis-related lncRNAs was performed, generating the common lncRNAs (Figure 2B). Finally, we obtained 48 lncRNAs which were significantly correlated with mitochondrial-related and ferroptosis-related lncRNAs (MF-related lncRNAs, Figure 2C).

Also, these MF-related lncRNAs were identified as potential prognostic indicators and were subjected to least absolute shrinkage and selection operator (LASSO) logistic regression algorithm analysis in the training cohort. Moreover, 10-fold cross-validation was also used for cross-validation. We identified 15 MF-related prognostic lncRNAs based on the min lambda (Figures 3A,B). Some 15 MF-related prognostic lncRNAs were enrolled into multivariate Cox regression analysis to further identify the prognostic lncRNAs. Finally, AC022007.1,

AC023090.1, AC099850.4, ACSL6-AS1, CYTOR, LHFPL3-AS2, AL365361.1, LINC02362, and MSC-AS1 were regarded as the MF-related and prognostic lncRNA (Figure 3C).

Validated the Expression of Mitochondrion and Ferroptosis-Related Prognostic Long Non-Coding RNA in the Independent Cohort

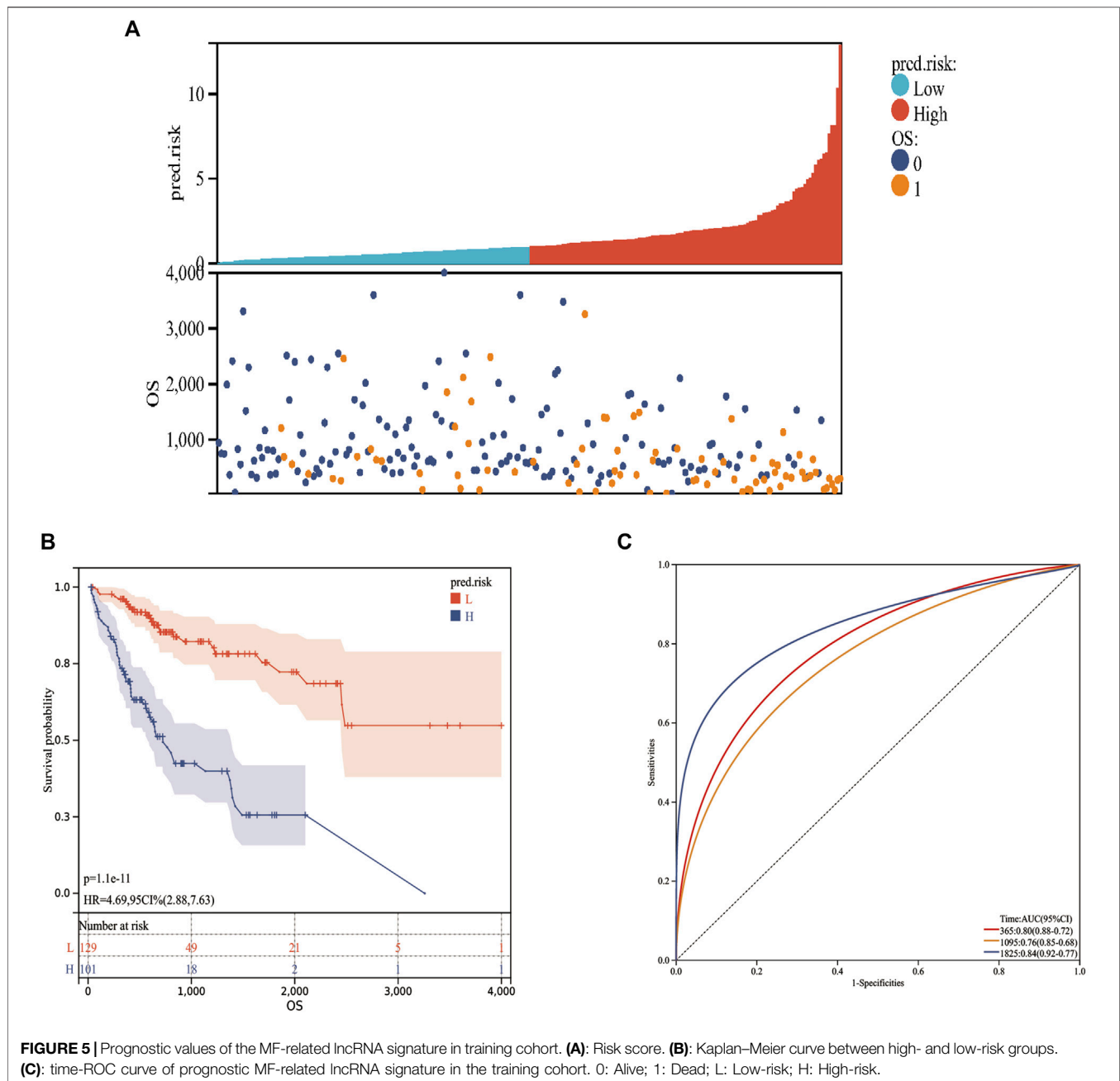
To further validate these prognostic lncRNA expression experimentally, 30 pairs of hepatocellular carcinoma tissues and adjacent normal liver tissues were selected from Guangdong Provincial People's Hospital and detected the nine lncRNA expression by RT-qPCR. We found that AC023090.1, AC099850.4, and CYTOR were significantly highly expressed in HCC tissues, while the expression of AL365361.1, AC022007.1, and LINC02362 was largely decreased in HCC tissues. The expression levels of MSC-ASL, LHFPL3-AS2, and ACSL6-AS1 were upregulated in the HCC sample though without statistically significant (Figure 4).



Construction and Evaluation of a Mitochondrion and Ferroptosis-Related Long Non-Coding RNA Prognostic Signature for LIHC Patients

Considering the expression of AC022007.1 in the TCGA cohort was opposite to the validation results of the GPDH cohort, a MF-related LPS was built based on the AC023090.1, AC099850.4, ACSL6-AS1, CYTOR, LHFPL3-AS2, AL365361.1, LINC02362, and MSC-AS1. The risk scores were calculated in the training cohort. The risk score of each patient could be calculated by the following formula: risk score = $(-0.16416 \times \text{expression value of AC023090.1}) + (0.37193 \times \text{expression value of AC099850.4}) + (-0.29628 \times \text{expression value of$

$\text{ACSL6-AS1}) + (-0.32870 \times \text{expression value of AL365361.1}) + (0.34095 \times \text{expression value of CYTOR}) + (-0.10062 \times \text{expression value of LHFPL3-AS2}) + (-0.12666 \times \text{expression value of LINC02362}) + (0.13118 \times \text{expression value of MSC-AS1})$. According to the best cutoff value of the risk scores, the training cohort can be divided into low-risk and high-risk groups (**Figure 5A**). Kaplan–Meier analysis was utilized to assess the stratification power of the MF-related LPS. The OS curve indicated that compared with low-risk group, the high-risk group had poorer OS (**Figure 5B**). Moreover, by using the time-dependent ROC curves, the MF-related LPS showed excellent accuracy in predicting 1-, 3-, and 5-year OS (1-year AUC = 0.80 3-year AUC = 0.76, 5-year OS = 0.84, **Figure 5C**).



Mitochondrion and Ferroptosis-Related Long Non-Coding RNA Prognostic Signature was an Independent Risk Factor for Overall Survival of the Training Cohort

Cox regression analysis was performed to identify the prognostic factors for LIHC patients. After removing the patients with unknown information and performing the univariate Cox regression analysis, MF-related LPS, tumor stage, and T stage were regarded as potential risk factors (Figure 6). All significant univariable predictors were enrolled into multivariate Cox regression analysis. Finally, the results indicated that MF-

related LPS and tumor stage were independent prognostic factors for overall survival (OS) in patients with hepatocellular carcinoma who underwent surgical therapy (Table2).

Validation of Mitochondrion and Ferroptosis-Related Long Non-Coding RNA Prognostic Signature in the Validation Cohort

Based on the MF-related LPS and the expression of each lncRNA from the validation cohort, the predicted risk scores were calculated. According to the best cutoff value

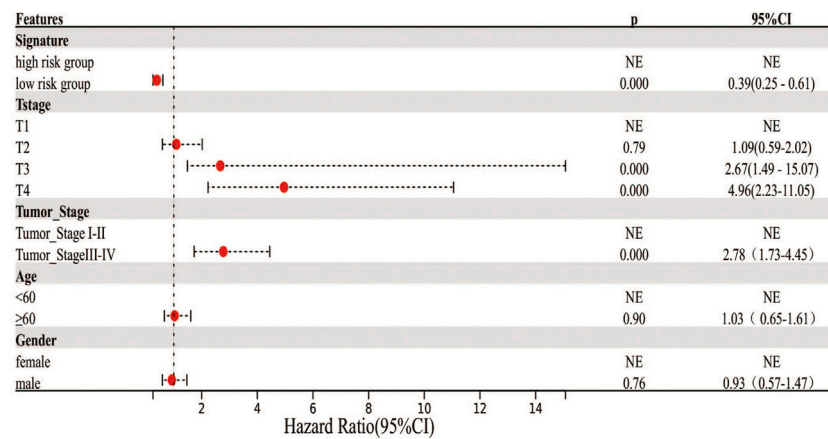


FIGURE 6 | Cox regression analysis on the clinicopathological factors and MF-related lncRNA signature. Forest plot showed the results of univariate Cox regression.

TABLE 2 | Multivariate Cox regression in the training cohort.

Features	HR	HR.95%L	HR.95H	p value	Hazard Ratio (95% CI)
Signature					
High-risk group				NE	
Low-risk group	0.39	0.25	0.61	<0.01	0.39 (0.25–0.61)
Tumor_stage					
I–II				NE	
III–IV	2.47	1.69	3.62	<0.01	2.47 (1.69–3.62)

from the training cohort, the validation population can also be divided into low-risk and high-risk groups (**Figure 7A**). Kaplan–Meier analysis validated the perfect stratification power of the MF-related LPS. The OS curve indicated that compared with the low-risk group, patients in the high-risk subgroup had worse survival (**Figure 7B**). As illustrated in **Figure 7C**, the AUC of MF-related LPS showed excellent accuracy in predicting 1-, 3-, and 5-year OS (1-year AUC = 0.72, 2-year AUC = 0.69, 5-year OS = 0.64). After performing the multivariate Cox regression analysis, the MF-related LPS was validated as the independent prognostic factors for overall survival (OS) in the validation cohort (**Table 3**).

The Association Between Mitochondrion and Ferroptosis-Related Long Non-Coding RNA Prognostic Signature and Clinicopathological Characteristics

We next performed association analysis to determine whether the MF-related LPS was related to clinicopathological characteristics in whole TCGA HCC patients. As **Table 4** indicated, there is no difference in age and gender between the high-risk group and low-risk group. But, there are more patients in the low-risk group with AJCC stage I–II, while there are more patients in the high-risk group with AJCC stage

III–IV. As for T stage, 130 patients at T1 stage are in the low-risk group and 77 patients at T2–T3 stage are in the high-risk group. Also, to further investigate the prognostic values of MF-related LPS in different subtypes of the TCGA LIHC population, subgroup analysis was conducted. The results revealed that the high-risk group is related to poorer OS in patients at early AJCC stage (I–II) or advanced AJCC stage (III–IV), patients with tumor stage T1, T2, or T3, and patients with age ≥ 60 or < 60 (**Supplementary Figure S1**).

Differentially Expressed Genes Between High- and Low-Risk Groups Were Identified and Function Enrichment Analysis Were Performed

To further investigate the differences between high- and low-risk groups, differential expression analysis was conducted by the *DESeq2* package. A total of 408 DEGs (upregulation: 308 and downregulation: 100) between two groups were identified ($p < 0.05$, $\text{Log}_2\text{FoldChange} > 1.0$, **Figure 8A**). Moreover, the DEGs between the high-risk and low-risk groups were used to perform GO enrichment and KEGG pathway analyses. GO component enrichment analysis showed that upregulated DEGs may be involved in “intrinsic component of plasma membrane, neuron projection, synapse, transporter complex,”

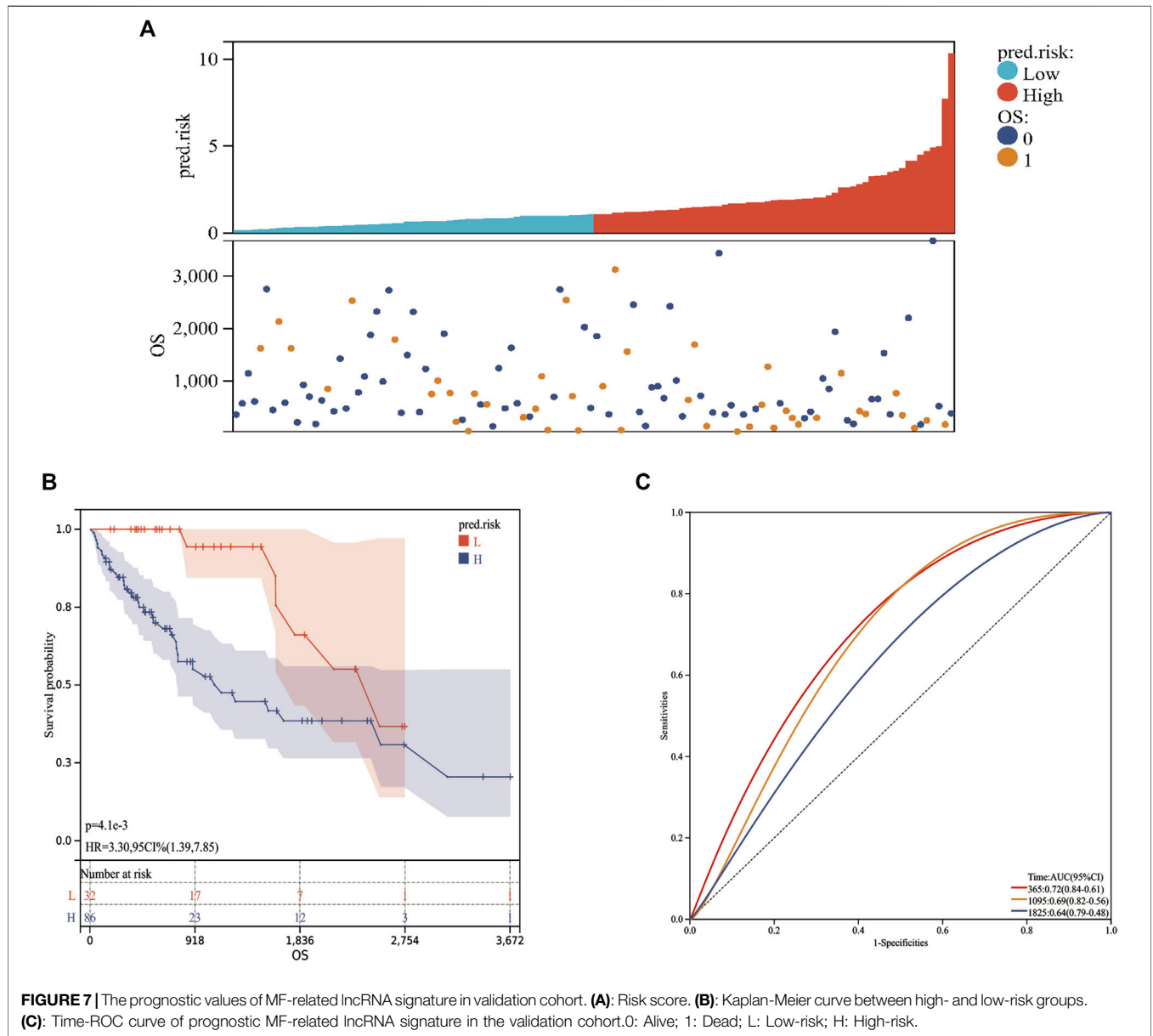


TABLE 3 | Multivariate Cox regression analysis in the validation cohort.

Features	HR	HR.95%L	HR.95%H	p value	Hazard Ratio (95% CI)
Signature					
High-risk group				NE	
Low-risk group	0.33	0.13	0.82	0.016	0.33 (0.13–0.82)
Tumor stage					
I-II				NE	
III-IV	1.06	0.14	7.96	0.96	1.06 (0.14–7.96)
Tstage					
T1				NE	
T2	1.62	0.85	3.07	0.14	1.62 (0.85–3.07)
T3	3.04	0.37	25.34	0.31	3.04 (0.37–25.34)
T4	1.06	0.04	11.81	0.79	1.06 (0.04–11.81)

TABLE 4 | Clinical characteristics of HCC patients in the high-risk group and low-risk group.

Characteristics	Low (n = 225)	High (n = 123)	p value
T stage			0.000041
T1	130 (57.78%)	39 (31.71%)	
T2	43 (19.11%)	43 (34.96%)	
T3	43 (19.11%)	34 (27.64%)	
T4	6 (2.67%)	7 (5.69%)	
unknown	3 (1.33%)	0 (0.0e + 0%)	
N stage			0.24
N0	152 (67.56%)	91 (73.98%)	
N1	3 (2.33%)	0 (0.0e + 0%)	
NX	70 (30.11%)	32 (26.02%)	
M stage			0.13
M0	154 (68.44%)	94 (76.42%)	
M1	4 (1.78%)	0 (0.0e + 0%)	
MX	67 (29.78%)	29 (23.58%)	
Tumor_stage			3.10E-04
stage I	123 (54.67%)	39 (31.71%)	
stage II	40 (17.78%)	38 (30.89%)	
stage III	45 (20%)	37 (30.08%)	
stage IV	4 (1.78%)	0 (0.0e + 0%)	
unknown	13 (5.77%)	9 (7.32%)	

etc., while downregulated DEGs may be involved in “synapse, secretory granule cell body,” etc. (Figure 8B). The GO biological process indicated that upregulated DEGs were mainly enriched in “neurogenesis, cell signaling, regulation of membrane potential,” etc., while the downregulated DEGs were mainly enriched in the “G protein-coupled receptor signaling pathway, positive regulation of cell population proliferation, antimicrobial humoral response,” etc. The GO molecular function indicated that upregulated DEGs may be involved in “passive transmembrane transporter activity, gated channel activity, neurotransmitter receptor activity,” etc. The downregulated DEGs were mainly enriched in “signaling receptor binding, receptor regulator activity, and hormone activity.” KEGG pathway analyses indicated that these upregulated genes were mainly involved in “neuroactive ligand-receptor interaction, cAMP signaling pathway, nicotine addiction, and retrograde endocannabinoid signaling.” (Figure 8C). GSEA analysis indicated that the “G2M checkpoint, E2F targets, MYC targets, GLYCOSIS signaling, etc.” were activated (Figure 8D).

Correlation Between the Mitochondrion- and Ferroptosis-Related Long Non-Coding RNA Prognostic Signature and Immune Cell Infiltration

To assess the relationship between immune cell infiltration and our MF-related LPS, we performed the ESTIMATE analysis. As shown in Figure 9A, the high-risk group had lower ESTIMATE score and immune score but had higher tumor purity than the low-risk group. Therefore, the EPIC analysis was performed to investigate the immune cell infiltration. As shown in Figure 9B, there were several different immune cell infiltrations between the high-risk and low-risk groups. The low-risk group had much more B cells, macrophages, CD 8+ T cell, and CD 4+ T cell

infiltration than the high-risk group. To further explore the correlation between the MF-related LPS and the infiltration of immune cell subtypes, the CIBERSORT algorithm was used. The results showed that the low-risk group had significant correlation with plasma cells, T cells, CD8 T cells, CD4 memory resting, while the high-risk group had significant correlation with regulatory T cells and M0 and M2 macrophages (Figure 9C).

DISCUSSIONS

Hepatocellular carcinoma is a common malignancy of the digestive system with difficulty in early diagnosis, high recurrence rate, and poor long-term survival. Therefore, it is urgent to figure out new therapeutic targets for hepatocellular carcinoma. LncRNAs are the important types of noncoding RNAs and can promote tumorigenesis, cell proliferation, migration, and metastasis by regulating gene expression on epigenetic modification. A growing number of studies show that mitochondrial dysfunction and ferroptosis are closely related to tumor progression. However, there is lack of systematic studies on the relations among lncRNAs, ferroptosis, and mitochondrial dysfunction and the mechanism of how to impact the fate of tumor cell and the immune cells.

In our study, we first obtain the mitochondria-related gene and ferroptosis-related genes from the previous studies. Also, after performing the Pearson analysis, the lncRNAs with the most significantly prognostic value and strongest correlation with mitochondria and ferroptosis were identified. The MF-related lncRNA-associated mitochondrial function defects and ferroptosis were further screened by Lasso-Cox regression.

Eight lncRNAs, namely, AC023090.1, AC099850.4, AL365361.1, CYTOR, ACSL6-AS1, LHFPL3-AS2, LINC02362, and MSC-AS1 were identified as the independent prognostic lncRNAs. Moreover, we verified the expression of these eight lncRNAs through RT-qPCR in our 30 pair samples from the GDPH cohort.

Previous study pointed out that AC099850.4 was one of the lncRNAs with most connections to miRNA or mRNA in High-Grade Serous Ovarian Cancer (Zhao et al., 2020). AL365361.1 was reported to improve the survival of head and neck squamous cell carcinoma, contributing to modification of the tumor microenvironment (Zhong et al., 2020). CYTOR and MSC-AS1 were highly expressed in many malignancies (Chen et al., 2021a; Chen et al., 2021b; Liu et al., 2021). Further studies had shown that CYTOR and MSC-AS1 inhibited the apoptosis of tumor cells and promoted EMT and tumor proliferation by acting as the ceRNAs for the miRNAs, such as miR-4775, miR-125B-5P (Hu et al., 2020; Chen et al., 2021b; Wang and Zhang, 2021; Liang et al., 2022). However, AC023090.1, ACSL6-AS1, LHFPL3-AS2, and LINC02362 are not mentioned in the previous research studies.

Based on these eight lncRNAs, we established the MF-related LPS. This LPS had very outstanding stratification ability. Patients can be divided into the high-risk group and low-risk group according to the risk scores calculated by the LPS. After further analysis, patients in the high-risk group tended to be at advanced T stage and AJCC stage and even with poorer overall survival. We also conducted the

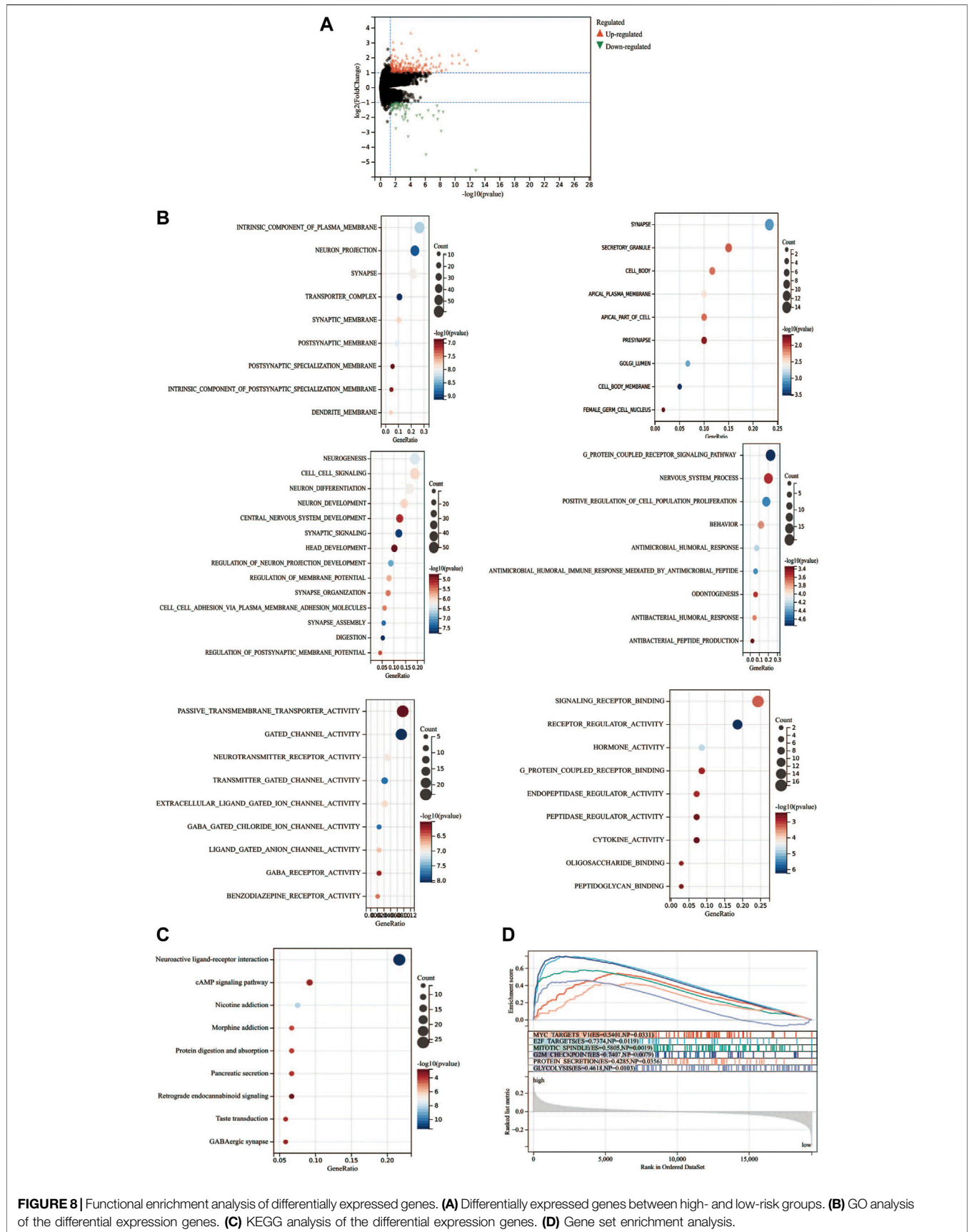
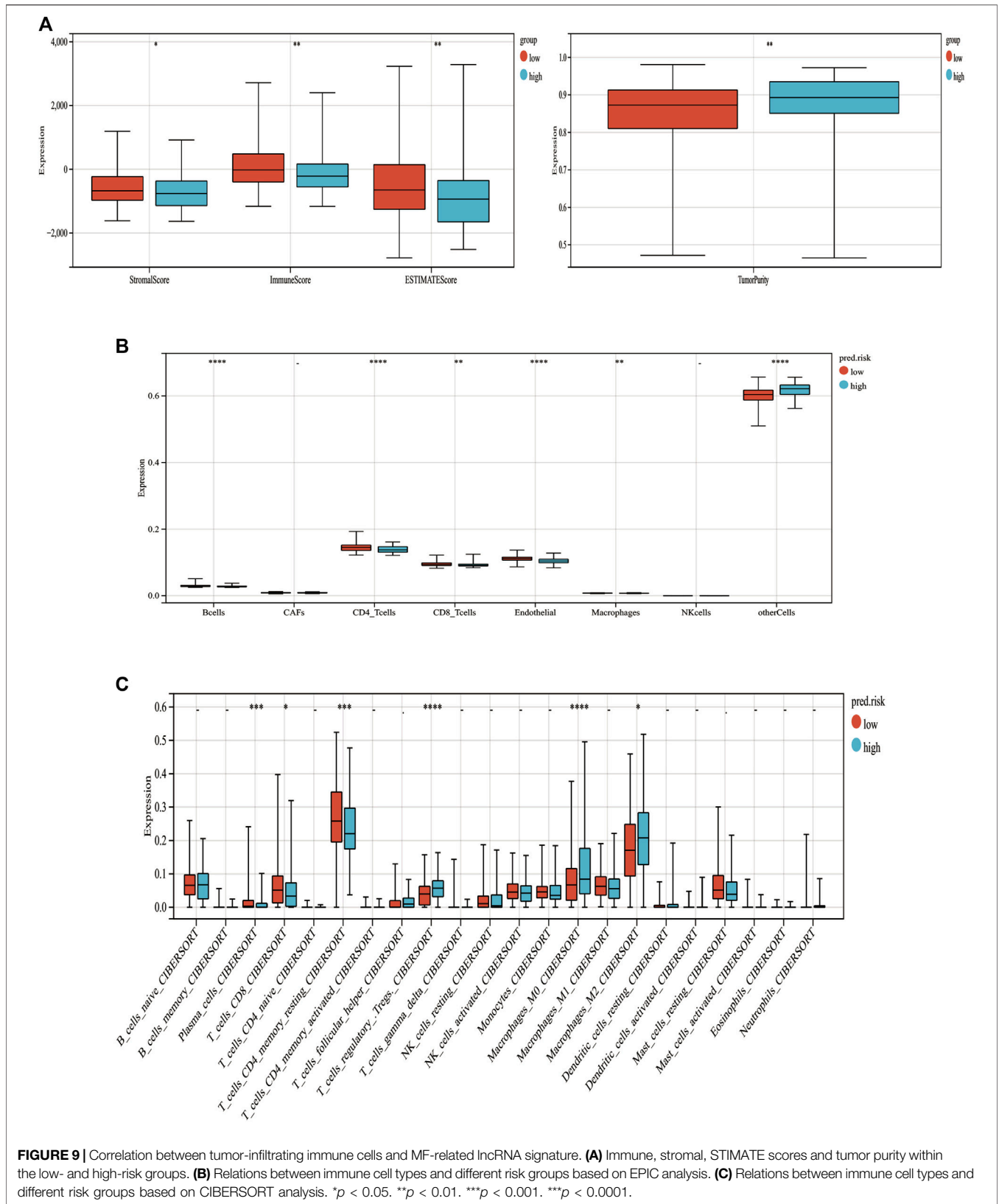


FIGURE 8 | Functional enrichment analysis of differentially expressed genes. **(A)** Differentially expressed genes between high- and low-risk groups. **(B)** GO analysis of the differential expression genes. **(C)** KEGG analysis of the differential expression genes. **(D)** Gene set enrichment analysis.



subgroup analysis, and LPS also had excellent stratification capabilities in different age, gender, T stage, and AJCC stage. We also found that LPS had very outstanding prognostic predictive capabilities, and 5-year AUC was 0.84. Moreover, based on 118 patients from TCGA cohorts, the stratification ability and prognostic prediction capability were fully validated.

Further functional enrichment analysis on the DEGs suggested that overexpressed genes in high-risk groups were associated with the signaling between cell and cell. GSEA results showed that the pathways related to tumorigenesis and tumor progression were significantly enriched in the high-risk group. These results indicated that these lncRNAs may affect mitochondria functions and ferroptosis in HCC through the cell cycle pathways.

Increasing immunosuppressive cells is one of the immune escape mechanisms which would make CD8⁺ T cells unable to identify the cancer cells and lead to tumor progression. Therefore, we analyzed the different immune cell infiltration between these two groups. Our studies have shown that these two groups had different immunocyte infiltration and tumor microenvironments. In our study, the infiltration ratio of regulatory T cells and M0 and M2 macrophages was higher in the high-risk group and the infiltration ratio of T cells CD8, CD4 memory resting, and monocytes was higher in the low-risk group. Studies reported that CD4 + T-cell help could enhance the response of CTLs (Borst et al., 2018) and patients with high CD4⁺ T cells infiltration were associated with better survival (Reyes et al., 2013). Mark Farha pointed out that the M0 macrophage-enriched group was a poor prognostic factor in HCC patients (Farha et al., 2020). Previous research studies revealed that M2 macrophages could promote the tumorigenesis by affecting the tumor microenvironment (Neophytou et al., 2021). A recent study indicated that a large number of Treg cells in the tumor microenvironment could inhibit the antitumor functions of human CD8⁺ T cells (Maeda et al., 2014). Also, high infiltration of Treg cells, in tumor microenvironment was related to poor prognosis (Tanaka and Sakaguchi, 2017).

In summary, our results suggested that AC023090.1, AC099850.4, AL365361.1, CYTOR, ACSL6-AS1, LHFPL3-AS2, LINC02362, and MSC-AS1 had the potential to be significant biomarkers. Also, we speculated these lncRNAs were regulating the mitochondria functions and ferroptosis through specific signaling pathways we mentioned above, which in turn influenced the tumorigenesis, cell proliferation, and differentiation. On the other hand, our research indicated that these lncRNAs are directly or indirectly regulating the tumor microenvironment by altering the infiltration or differentiation of immune cells and promoted tumor progression.

Despite the important findings, there is no denying that this study has several limitations. First, the data were collected from the online public datasets with few clinicopathological data, potential errors, or deviations that should be considered. Second, some verification results in the GDPH cohort would not be statistically significant because of the small sample size, and further independent and large number cohorts are needed to validate our findings in future. In addition, the molecular mechanisms on how these lncRNAs function must be explored further through fundamental experiments.

CONCLUSION

To conclude, based on the nine mitochondria and ferroptosis-related lncRNAs, a MF-related LPS was built successfully. More importantly, we found that these lncRNAs may affect mitochondrial functions, ferroptosis, and immune cell infiltration in HCC through specific pathways, which may provide valuable insight on the progression and therapies of HCC.

DATA AVAILABILITY STATEMENT

The datasets TCGA (<https://portal.gdc.cancer.gov/>) for this study can be found in the websites. And further inquiries can be directed to the corresponding authors.

ETHICS STATEMENT

The studies involving human participants were reviewed and approved by the Guangdong Provincial People's Hospital. The patients/participants provided their written informed consent to participate in this study.

AUTHOR CONTRIBUTIONS

ZZ, WX, CZ, and LB conceived and designed the study. ZZ performed the bioinformatics analysis and interpreted the results. WX and CZ performed the RT-PCR and interpreted the results of PCR. All drafts of the reports were written by ZZ, CZ, and CH. All authors read and approved the final version of the manuscript. WX, CZ, and ZZ contributed equally to this work.

FUNDING

The current study is supported by the National Natural Science Foundation of China (grant no. 81970451), the Natural Science Foundation of Guangdong Province (grant nos. 2021A1515010013 and 2019A1515010667), the Clinical Research Startup Program of Southern Medical University by High-level University Construction Funding of Guangdong Provincial Department of Education (grant no. LC2019ZD021), National key Clinical Specialty Construction Project (2021-2024, No. 2022YW030009 and the Clinical Research Program of Nanfang Hospital, Southern Medical University (grant nos. 2020CR027 and 2018CR038).

SUPPLEMENTARY MATERIAL

The Supplementary Material for this article can be found online at: <https://www.frontiersin.org/articles/10.3389/fcell.2022.844759/full#supplementary-material>

Supplementary Figure S1 | Association between MF-related LPS and clinicopathological characteristics.

REFERENCES

- Ahadi, A. (2021). Functional Roles of lncRNAs in the Pathogenesis and Progression of Cancer. *Genes. & Dis.* 8, 424–437. doi:10.1016/j.gendis.2020.04.009
- Bahat, A., and Gross, A. (2019). Mitochondrial Plasticity in Cell Fate Regulation. *J. Biol. Chem.* 294, 13852–13863. doi:10.1074/jbc.REV118.000828
- Benson, A. B. (2021). Hepatobiliary Cancers, Version 2.2021, NCCN Clinical Practice Guidelines in Oncology. *J. Natl. Compr. Canc Netw.* 19, 541–565. doi:10.6004/jnccn.2021.0022
- Borst, J., Ahrends, T., Bąbala, N., Melief, C. J. M., and Kastentmüller, W. (2018). CD4+ T Cell Help in Cancer Immunology and Immunotherapy. *Nat. Rev. Immunol.* 18, 635–647. doi:10.1038/s41577-018-0044-0
- Bruix, J., Reig, M., and Sherman, M. (2016). Evidence-Based Diagnosis, Staging, and Treatment of Patients with Hepatocellular Carcinoma. *Gastroenterology* 150, 835–853. doi:10.1053/j.gastro.2015.12.041
- Chen, B., Khodadoust, M. S., Liu, C. L., Newman, A. M., and Alizadeh, A. A. (2018). Profiling Tumor Infiltrating Immune Cells with CIBERSORT. *Methods Mol. Biol.* 1711, 243–259. doi:10.1007/978-1-4939-7493-1_12
- Chen, S., Yang, M., Wang, C., Ouyang, Y., Chen, X., Bai, J., et al. (2021). Forkhead Box D1 Promotes EMT and Chemoresistance by Upregulating lncRNA CYTOR in Oral Squamous Cell Carcinoma. *Cancer Lett.* 503, 43–53. doi:10.1016/j.canlet.2020.11.046
- Chen, Z.-A., Tian, H., Yao, D.-M., Zhang, Y., Feng, Z.-J., and Yang, C.-J. (2021). Identification of a Ferroptosis-Related Signature Model Including mRNAs and lncRNAs for Predicting Prognosis and Immune Activity in Hepatocellular Carcinoma. *Front. Oncol.* 11, 738477. doi:10.3389/fonc.2021.738477
- Dhanoa, J. K., Sethi, R. S., Verma, R., Arora, J. S., and Mukhopadhyay, C. S. (2018). Long Non-coding RNA: its Evolutionary Relics and Biological Implications in Mammals: a Review. *J. Anim. Sci. Technol.* 60, 25. doi:10.1186/s40781-018-0183-7
- Du, X., and Zhang, Y. (2020). Integrated Analysis of Immunity- and Ferroptosis-Related Biomarker Signatures to Improve the Prognosis Prediction of Hepatocellular Carcinoma. *Front. Genet.* 11, 614888. doi:10.3389/fgene.2020.614888
- Engelbrechtsen, S., and Bohlin, J. (2019). Statistical Predictions with Glimnet. *Clin. Epigenet* 11, 123. doi:10.1186/s13148-019-0730-1
- Farha, M., Jairath, N. K., Lawrence, T. S., and El Naqa, I. (2020). Characterization of the Tumor Immune Microenvironment Identifies M0 Macrophage-Enriched Cluster as a Poor Prognostic Factor in Hepatocellular Carcinoma. *JCO Clin. Cancer Inf.* 4, 1002–1013. doi:10.1200/CCL.20.00077
- Frankish, A., Diekhans, M., Ferreira, A.-M., Johnson, R., Jungreis, I., Loveland, J., et al. (2019). GENCODE Reference Annotation for the Human and Mouse Genomes. *Nucleic Acids Res.* 47, D766–D773. doi:10.1093/nar/gky955
- Gai, C., Liu, C., Wu, X., Yu, M., Zheng, J., Zhang, W., et al. (2020). MT1DP Loaded by Folate-Modified Liposomes Sensitizes Erastin-Induced Ferroptosis via Regulating miR-365a-3p/NRF2 axis in Non-small Cell Lung Cancer Cells. *Cell. Death Dis.* 11, 751. doi:10.1038/s41419-020-02939-3
- Gao, M., Yi, J., Zhu, J., Minikes, A. M., Monian, P., Thompson, C. B., et al. (2019). Role of Mitochondria in Ferroptosis. *Mol. Cell.* 73, 354–363. e353. doi:10.1016/j.molcel.2018.10.042
- Hassannia, B., Vandenabeele, P., and Vanden Berghe, T. (2019). Targeting Ferroptosis to Iron Out Cancer. *Cancer Cell.* 35, 830–849. doi:10.1016/j.ccell.2019.04.002
- Heimbach, J. K., Kulik, L. M., Finn, R. S., Sirlin, C. B., Abecassis, M. M., Roberts, L. R., et al. (2018). AASLD Guidelines for the Treatment of Hepatocellular Carcinoma. *Hepatology* 67, 358–380. doi:10.1002/hep.29086
- Hu, B., Yang, X.-B., Yang, X., and Sang, X.-T. (2020). lncRNA CYTOR Affects the Proliferation, Cell Cycle and Apoptosis of Hepatocellular Carcinoma Cells by Regulating the miR-125b-5p/KIAA1522 axis. *Aging* 13, 2626–2639. doi:10.18632/aging.202306
- Ishizawa, T., Hasegawa, K., Aoki, T., Takahashi, M., Inoue, Y., Sano, K., et al. (2008). Neither multiple Tumors Nor Portal Hypertension Are Surgical Contraindications for Hepatocellular Carcinoma. *Gastroenterology* 134, 1908–1916. doi:10.1053/j.gastro.2008.02.091
- Lanzafame, M., Bianco, G., Terracciano, L., Ng, C., and Piscuoglio, S. (2018). The Role of Long Non-coding RNAs in Hepatocarcinogenesis. *Ijms* 19, 682. doi:10.3390/ijms19030682
- Lencioni, R., de Baere, T., Soulen, M. C., Rilling, W. S., and Geschwind, J.-F. H. (2016). Lipiodol Transarterial Chemoembolization for Hepatocellular Carcinoma: A Systematic Review of Efficacy and Safety Data. *Hepatology* 64, 106–116. doi:10.1002/hep.28453
- Li, C., Zhang, Y., Liu, J., Kang, R., Klionsky, D. J., and Tang, D. (2021). Mitochondrial DNA Stress Triggers Autophagy-dependent Ferroptotic Death. *Autophagy* 17, 948–960. doi:10.1080/15548627.2020.1739447
- Li, H., Slone, J., and Huang, T. (2020). The Role of Mitochondrial-Related Nuclear Genes in Age-Related Common Disease. *Mitochondrion* 53, 38–47. doi:10.1016/j.mito.2020.04.012
- Liang, C., Wang, J., Liu, A., and Wu, Y. (2022). Tumor Promoting Long Non-coding RNA CASC15 Affects HMGB2 Expression by Sponging miR-582-5p in Colorectal Cancer. *J. Gene Med.* 24, e3308. doi:10.1002/jgm.3308
- Liu, Y., Li, L., Wu, X., Qi, H., Gao, Y., Li, Y., et al. (2021). MSC-AS1 Induced Cell Growth and Inflammatory Mediators Secretion through Sponging miR-142-5p/DDX5 in Gastric Carcinoma. *Aging* 13, 10387–10395. doi:10.18632/aging.202800
- Love, M. I., Huber, W., and Anders, S. (2014). Moderated Estimation of Fold Change and Dispersion for RNA-Seq Data with DESeq2. *Genome Biol.* 15, 550. doi:10.1186/s13059-014-0550-8
- Maeda, Y., Nishikawa, H., Sugiyama, D., Ha, D., Hamaguchi, M., Saito, T., et al. (2014). Detection of Self-Reactive CD8+ T Cells with an Anergic Phenotype in Healthy Individuals. *Science* 346, 1536–1540. doi:10.1126/science.aaa1292
- Manz, D. H., Blanchette, N. L., Paul, B. T., Torti, F. M., and Torti, S. V. (2016). Iron and Cancer: Recent Insights. *Ann. N.Y. Acad. Sci.* 1368, 149–161. doi:10.1111/nyas.13008
- Nandwani, A., Rathore, S., and Datta, M. (2021). lncRNAs in Cancer: Regulatory and Therapeutic Implications. *Cancer Lett.* 501, 162–171. doi:10.1016/j.canlet.2020.11.048
- Neophytou, C. M., Panagi, M., Stylianopoulos, T., and Papageorgis, P. (2021). The Role of Tumor Microenvironment in Cancer Metastasis: Molecular Mechanisms and Therapeutic Opportunities. *Cancers* 13, 2053. doi:10.3390/cancers13092053
- Petrick, J. L., Braunlin, M., Laversanne, M., Valery, P. C., Bray, F., and McGlynn, K. A. (2016). International Trends in Liver Cancer Incidence, Overall and by Histologic Subtype, 1978–2007. *Int. J. Cancer* 139, 1534–1545. doi:10.1002/ijc.30211
- Prensner, J. R., and Chinnaiyan, A. M. (2011). The Emergence of lncRNAs in Cancer Biology. *Cancer Discov.* 1, 391–407. doi:10.1158/2159-8290.CD-11-0209
- Racle, J., and Gfeller, D. (2020). EPIC: A Tool to Estimate the Proportions of Different Cell Types from Bulk Gene Expression Data. *Methods Mol. Biol.* 2120, 233–248. doi:10.1007/978-1-0716-0327-7_17
- Rath, S., Sharma, R., Gupta, R., Ast, T., Chan, C., Durham, T. J., et al. (2021). MitoCarta3.0: an Updated Mitochondrial Proteome Now with Sub-organelle Localization and Pathway Annotations. *Nucleic Acids Res.* 49, D1541–D1547. doi:10.1093/nar/gkaa1011
- Reyes, D., Salazar, L., Espinoza, E., Pereda, C., Castellón, E., Valdevenito, R., et al. (2013). Tumour Cell Lysate-Loaded Dendritic Cell Vaccine Induces Biochemical and Memory Immune Response in Castration-Resistant Prostate Cancer Patients. *Br. J. Cancer* 109, 1488–1497. doi:10.1038/bjc.2013.494
- Shyh-Chang, N., Daley, G. Q., and Cantley, L. C. (2013). Stem Cell Metabolism in Tissue Development and Aging. *Development* 140, 2535–2547. doi:10.1242/dev.091777
- Stockwell, B. R., Friedmann Angeli, J. P., Bayir, H., Bush, A. I., Conrad, M., Dixon, S. J., et al. (2017). Ferroptosis: A Regulated Cell Death Nexus Linking Metabolism, Redox Biology, and Disease. *Cell* 171, 273–285. doi:10.1016/j.cell.2017.09.021
- Tanaka, A., and Sakaguchi, S. (2017). Regulatory T Cells in Cancer Immunotherapy. *Cell. Res.* 27, 109–118. doi:10.1038/cr.2016.151
- Tang, D., Chen, X., Kang, R., and Kroemer, G. (2021). Ferroptosis: Molecular Mechanisms and Health Implications. *Cell. Res.* 31, 107–125. doi:10.1038/s41422-020-00441-1
- Tibshirani, R. (1997). The Lasso Method for Variable Selection in the Cox Model. *Stat. Med.* 16, 385–395. doi:10.1002/(sici)1097-0258(19970228)16:4<385::aid-sim380>3.0.co;2-3

- Uszczynska-Ratajczak, B., Lagarde, J., Frankish, A., Guigó, R., and Johnson, R. (2018). Towards a Complete Map of the Human Long Non-coding RNA Transcriptome. *Nat. Rev. Genet.* 19, 535–548. doi:10.1038/s41576-018-0017-y
- Wang, H., and Zhang, P. (2021). lncRNA-CASC15 Promotes O-steosarcoma Proliferation and Metastasis by Regulating E-pithelial-mesenchymal Transition via the Wnt/ β -catenin Signaling Pathway. *Oncol. Rep.* 45. doi:10.3892/or.2021.8027
- Yang, J.-F., Shi, S.-N., Xu, W.-H., Qiu, Y.-H., Zheng, J.-Z., Yu, K., et al. (2019). Screening, Identification and Validation of CCND1 and PECAM1/CD31 for Predicting Prognosis in Renal Cell Carcinoma Patients. *Aging* 11, 12057–12079. doi:10.18632/aging.102540
- Yu, G., Wang, L.-G., Han, Y., and He, Q.-Y. (2012). clusterProfiler: an R Package for Comparing Biological Themes Among Gene Clusters. *OMICS A J. Integr. Biol.* 16, 284–287. doi:10.1089/omi.2011.0118
- Yuan, Y., Ju, Y. S., Kim, Y., Li, J., Wang, Y., Yoon, C. J., et al. (2020). Comprehensive Molecular Characterization of Mitochondrial Genomes in Human Cancers. *Nat. Genet.* 52, 342–352. doi:10.1038/s41588-019-0557-x
- Zhang, Q., Ning, G., Jiang, H., Huang, Y., Piao, J., Chen, Z., et al. (2020). 15-lncRNA-Based Classifier-Clinicopathologic Nomogram Improves the Prediction of Recurrence in Patients with Hepatocellular Carcinoma. *Dis. Markers* 2020, 15. doi:10.1155/2020/9180732
- Zhao, J., Song, X., Xu, T., Yang, Q., Liu, J., Jiang, B., et al. (2020). Identification of Potential Prognostic Competing Triplets in High-Grade Serous Ovarian Cancer. *Front. Genet.* 11, 607722. doi:10.3389/fgene.2020.607722
- Zhao, Y., Zhou, L., Li, H., Sun, T., Wen, X., Li, X., et al. (2021). Nuclear-Encoded lncRNA MALAT1 Epigenetically Controls Metabolic Reprogramming in HCC Cells through the Mitophagy Pathway. *Mol. Ther. - Nucleic Acids* 23, 264–276. doi:10.1016/j.omtn.2020.09.040
- Wang, W., Sun, Q., Wu, Z., Zhou, D., Wei, J., Xie, H., et al. (2013). Mitochondrial Dysfunction-Related Genes in Hepatocellular Carcinoma. *Front. Biosci.* 18 (3), 1141–1149. doi:10.2741/4169
- Zhong, Z., Hong, M., Chen, X., Xi, Y., Xu, Y., Kong, D., et al. (2020). Transcriptome Analysis Reveals the Link between lncRNA-mRNA Co-expression Network and Tumor Immune Microenvironment and Overall Survival in Head and Neck Squamous Cell Carcinoma. *BMC Med. Genomics* 13, 57. doi:10.1186/s12920-020-0707-0
- Zhou, J., Sun, H., Wang, Z., Cong, W., Wang, J., Zeng, M., et al. (2019). Guidelines for the Diagnosis and Treatment of Hepatocellular Carcinoma (2019 Edition). *Liver Cancer* 9, 682–720. doi:10.1159/000509424
- Zhou, M., Wang, H., Zeng, X., Yin, P., Zhu, J., Chen, W., et al. (2019). Mortality, Morbidity, and Risk Factors in China and its Provinces, 1990–2017: a Systematic Analysis for the Global Burden of Disease Study 2017. *Lancet* 394, 1145–1158. doi:10.1016/S0140-6736(19)30427-1
- Zhou, R., Liang, J., Tian, H., Chen, Q., Yang, C., and Liu, C. (2021). Development of a Ferroptosis-Related lncRNA Signature to Predict the Prognosis and Immune Landscape of Bladder Cancer. *Dis. Markers* 2021, 22. doi:10.1155/2021/1031906
- Zong, W. X., Rabinowitz, J. D., and White, E. (2016). Mitochondria and Cancer. *Mol. Cell.* 61, 667–676. doi:10.1016/j.molcel.2016.02.011

Conflict of Interest: The authors declare that the research was conducted in the absence of any commercial or financial relationships that could be construed as a potential conflict of interest.

Publisher's Note: All claims expressed in this article are solely those of the authors and do not necessarily represent those of their affiliated organizations, or those of the publisher, the editors, and the reviewers. Any product that may be evaluated in this article, or claim that may be made by its manufacturer, is not guaranteed or endorsed by the publisher.

Copyright © 2022 Xia, Zeng, Zheng, Huang, Zhou and Bai. This is an open-access article distributed under the terms of the Creative Commons Attribution License (CC BY). The use, distribution or reproduction in other forums is permitted, provided the original author(s) and the copyright owner(s) are credited and that the original publication in this journal is cited, in accordance with accepted academic practice. No use, distribution or reproduction is permitted which does not comply with these terms.